GEOFLUIDS

Geofluids (2015) **15**, 1–10 doi: 10.1111/gfl.12118

Crustal permeability: Introduction to the special issue

S. E. INGEBRITSEN[1] AND T. GLEESON[2]

[1]*U.S. Geological Survey, Menlo Park, CA, USA;* [2]*Civil Engineering Department, McGill University, Montreal, Quebec, Canada*

Received 16 June 2014; accepted 23 September 2014

Corresponding author: Steve Ingebritsen, U.S. Geological Survey, Menlo Park, CA 94025, USA. Email: seingebr@usgs.gov.Tel: 650 329 4422. Fax: 650 329 4463.

Geofluids (2015) **15**, 1–10

MOTIVATION AND BACKGROUND

The topic of crustal permeability is of broad interest in light of the controlling effect of permeability on diverse geologic processes and also timely in light of the practical challenges associated with emerging technologies such as hydraulic fracturing for oil and gas production ('fracking'), enhanced geothermal systems, and geologic carbon sequestration. This special issue of *Geofluids* is also motivated by the historical dichotomy between the hydrogeologic concept of permeability as a static material property that exerts control on fluid flow and the perspective of economic geologists, geophysicists, and crustal petrologists who have long recognized permeability as a dynamic parameter that changes in response to tectonism, fluid production, and geochemical reactions. Issues associated with fracking, enhanced geothermal systems, and geologic carbon sequestration have already begun to promote a constructive dialog between the static and dynamic views of permeability, and here we have made a conscious effort to include both viewpoints. This special issue also focuses on the quantification of permeability, encompassing both direct measurement of permeability in the uppermost crust and inferential permeability estimates, mainly for the deeper crust.

The directly measured permeability (k) of common geologic media varies by approximately 16 orders of magnitude, from values as low as 10^{-23} m^2 in intact crystalline rock, intact shales, and fault gouge, to values as high as 10^{-7} m^2 in well-sorted gravels. The permeability of Earth's upper crust can be regarded as a process-limiting parameter, in that it largely determines the feasibility of advective solute transport ($k \sim >10^{-20}$ m^2), advective heat transport ($k \sim \geq 10^{-16}$ m^2), and the generation of elevated fluid pressures ($k \sim \leq 10^{-17}$ m^2) – processes which in turn are essential to ore deposition, hydrocarbon migration, metamorphism, tectonism, and many other fundamental geologic phenomena.

The hydrodynamics of fluids in the brittle upper crust, where topography and magmatic heat sources dominate patterns of flow and externally derived (meteoric) fluids are common (e.g. Howald *et al.* 2015) are distinct from the ductile lower crust, dominated by devolatilization reactions and internally derived fluids (e.g. Connolly & Podladchikov, 2015). The brittle–ductile transition between these regimes occurs at 10–15 km depth in typical continental crust. Permeability below the brittle–ductile transition is non-negligible, at least in active orogenic belts (equivalent to mean bulk k of order 10^{-19} to 10^{-18} m^2) so that the underlying ductile regime can be an important fluid source to the brittle regime (e.g. Ingebritsen & Manning 2002). The overall objective of this special issue is to synthesize current understanding of static and dynamic permeability through representative publications from multiple disciplines.

The objective of this introduction to the special issue is to define crucial nomenclature and the 'static' and 'dynamic' permeability perspectives and to briefly summarize the contents of this special issue, which is divided into the following sections: the physics of permeability, static permeability, and dynamic permeability.

NOMENCLATURE: POROSITY, PERMEABILITY, HYDRAULIC CONDUCTIVITY, AND RELATIVE PERMEABILITY

For the benefit of the broad *Geofluids* community, which includes scientists from a wide range of disciplinary backgrounds, we briefly define some of the key hydrogeologic parameters that are repeatedly used in this special issue, namely porosity, permeability, hydraulic conductivity, and relative permeability. These are conceptually related but distinct concepts.

First, we note that all of these parameters are continuum properties that are only definable on a macroscopic scale.

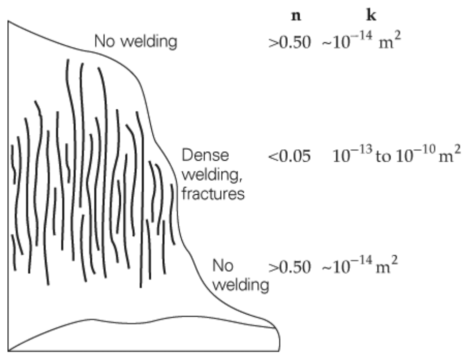

Fig. 1. Cross-section through a hypothetical ash-flow tuff unit showing typical values of porosity (*n*) and permeability (*k*). The thickness of individual ash-flow tuff sheets ranges from a few meters to over 300 m. Tertiary ash-flow tuffs are widespread in the Western United States, particularly in the Basin and Range province. After Winograd (1971).

Perhaps most obviously, at any microscopic point in a domain, porosity ($V_{\mathrm{void}}/V_{\mathrm{total}} = n$) will be either 0 in the solid material or 1 in a pore space. As one averages over progressively larger volumes, the computed value of n will vary between 0 and 1 and, if the medium is sufficiently homogeneous, the volume-averaged value of n will eventually become nearly constant over a volume range which has been termed the representative elementary volume or (REV) (Bear 1972, 1979). Figure 1 shows, for example, a hypothetical section of volcanic ash-flow tuff; note the distinctly different porosity of the flow center relative to the flow top and bottom. The concept of permeability – the ability of a material to transmit fluid – also applies only at an REV scale and can be regarded as reflecting detailed solid–fluid geometries that we cannot map and thus wish to render as large-scale properties. Exact analytical expressions for permeability can be obtained for simple geometries such as bundles of capillary tubes or parallel plates (constant-aperture fractures), but actual pore-fracture geometries are never known.

Porosity (n) – permeability (k) relations have been the subject of many studies (e.g. Luijendijk & Gleeson, 2015), and there is often a positive correlation between these two essential quantities. However, even in the case of classical porous media, a correlation between n and k cannot be assumed for mixed size grains, or when comparing media with greatly different grain sizes. For instance, although there is a positive correlation between n and k for clays themselves, clays are 10^4–10^{10} times less permeable than well-sorted sands (e.g. Freeze & Cherry 1979), despite having generally higher porosities. Further, positive correlation between n and k cannot be assumed in more complex media. Consider again our ash-flow tuff example (Fig. 1): the top and bottom of an ash flow cool relatively rapidly, retaining their original high porosities (approximately 0.50), but the permeability of this 'unwelded' material is relatively low, because the pores are small and not well connected. If the ash flow is sufficiently thick, pores deform and collapse in the slowly cooling interior, where the final value of porosity can be quite low (<0.05). However, the flow interior also tends to fracture during cooling, and the interconnected fractures transmit water very effectively despite the low overall porosity. The net result of the cooling history is that flow interiors typically have up to 10^4 times higher permeability than 'unwelded' flow tops and bottoms, despite their much lower porosities (0.05 versus 0.50).

Both laboratory and *in situ* (borehole) testing normally return values of hydraulic conductivity (K) rather than permeability (k), and this parameter reflects both rock and fluid properties:

$$K = \frac{k\rho_{\mathrm{f}}g}{\mu_{\mathrm{f}}},$$

where $\rho_{\mathrm{f}}g$ gis the specific weight of the fluid and μ_{f} is its dynamic viscosity. In order to compare rock properties among different geothermal conditions, or different fluids (e.g. hydrocarbons versus aqueous fluids), it is necessary to convert measured values of K to values of k (e.g. Stober & Bucher, 2015). Considering once again our ash-flow tuff example: if the surficial outcrop depicted in Fig. 1 could somehow be translated from standard temperature and pressure (STP = 15°C, 1 bar) to 300°C and approximately 1000 bars (approximately 10 km depth), without any changes in its physical morphology, its permeability k would not change, but its hydraulic conductivity would be approximately 10 times larger because of the increase in the $\rho_{\mathrm{f}}/\mu_{\mathrm{f}}$ ratio.

Finally, the empirically based concept of relative permeability is used to extend the linear flow law for viscous fluids (*i.e.* Darcy's law) to multiphase systems. Relative permeability (k_{r}) represents the reduction in the mobility of one fluid phase due to the interfering presence of another fluid phase in the void space and is treated as a scalar varying from 0 to 1, usually as some function of volumetric saturation (e.g. $V_{\mathrm{liquid}}/V_{\mathrm{void}}$, where for instance $[V_{\mathrm{vapor}} + V_{\mathrm{liquid}}]/V_{\mathrm{void}} = 1$). This concept is widely invoked in the context of hydrocarbon migration and production (oil–gas-–liquid water) and unsaturated flow above the water table (air–liquid water), but is also applied to multiphase flow in hydrothermal systems – for instance by Weis (2015), who allows for the presence of three distinct phases in the void space (vapor + liquid + solid NaCl). Because methane-saturated shales can have very low permeabilities to basinal brines, some studies have used relative-permeability effects to explain anomalous pressure in mature sedimentary basins (e.g. Deming *et al.* 2002).

STATIC VERSUS DYNAMIC PERMEABILITY

Some economic geologists, geophysicists, and metamorphic petrologists have long recognized permeability as a dynamic parameter that changes in response to dewatering, fluid production, and seismicity (e.g. Sibson *et al.* 1975;

Walder & Nur 1984; Yardley 1986; Hanson 1995; Connolly 1997). For purposes of this special issue, we consider 'dynamic permeability' to include any transient variations in permeability, regardless of timescale. However, as pointed out by Huber & Su (2015), 'dynamic permeability' also has a traditional and much narrower technical definition as frequency-dependent permeability.

The view of permeability as a dynamic parameter varying with time is in stark contrast to the hydrogeologic concept of permeability as a static material property that exerts control on fluid flow. Indeed, the term 'intrinsic permeability', widely used in the hydrogeologic and petroleum-engineering literature, seems to imply an immutable property.

However, there is abundant evidence that permeability varies in time as well as space, and that temporal variability in permeability is particularly pronounced in environments characterized by strong chemical and thermal disequilibrium. Laboratory experiments involving hydrothermal flow in crystalline rocks under pressure, temperature, and chemistry gradients often result in order-of-magnitude permeability decreases over daily to subannual timescales (e.g. Morrow *et al.* 1981; Moore *et al.* 1994; Yasuhara *et al.* 2006), and field observations of continuous, cyclic and episodic hydrothermal-flow transients at various timescales also suggest transient variations in permeability (e.g. Baker *et al.* 1987; Hill *et al.* 1993; Haymon 1996; Fornari *et al.* 1998; Sohn 2007). The occurrence of active, long-lived (10^3–10^6 years) hydrothermal systems (Cathles *et al.* 1997), despite the tendency for permeability to decrease with time, implies that other processes such as hydraulic fracturing and earthquakes regularly create new flow paths (e.g. Rojstaczer *et al.* 1995). Indeed, in the past decade, coseismic permeability enhancement and subsequent permeability decay have been directly observed (Elkhoury *et al.* 2006; Kitagawa *et al.* 2007; Xue *et al.* 2013). It is also clear that sufficiently overpressured fluids cannot be contained in the crust and will create the permeability necessary to escape (e.g. Cathles & Adams 2005; Connolly & Podladchikov 2015; Weis, 2015). These various observations have inspired suggestions that crustal-scale permeability is a dynamically self-adjusting or even emergent property (e.g. Townend & Zoback 2000; Rojstaczer *et al.* 2008; Weis *et al.* 2012), reflecting a dynamic competition between permeability creation by processes such as fluid sourcing and tectonic fracturing and permeability destruction by processes such as compaction, diagenesis, hydrothermal alteration, and retrograde metamorphism.

CONTENTS OF THE SPECIAL ISSUE

The contents of this special issue can be broadly categorized as dealing with the physics of permeability (4 papers), static permeability (6 papers), and dynamic permeability (11 papers). The final contribution proposes a data structure to embrace and extend existing knowledge of crustal permeability.

The physics of permeability

Darcy's law is an expression of conservation of momentum that describes viscous fluid flow through a porous medium. It provides the scientific basis for the concept of permeability. The first two papers in this collection explore limits to the validity of Darcy's law. For porous media subjected to harmonic pressure forcing, the effective permeability is frequency dependent, an effect that has classically been represented as a dynamic correction to the effective fluid viscosity and has been termed 'dynamic permeability' (a term that we define more broadly here). This results from the fact that Darcy's law (and therefore permeability) was originally developed for cases where inertial forces are negligible. When inertial forces are significant, the ratio of fluid flux to pressure gradient may not be constant. The seminal model of Johnson *et al.* (1987) (JKD) defined a critical frequency that represents the transition from viscous- to inertia-dominated momentum balance in homogeneous porous media. Lattice-Boltzmann simulations by Huber & Su (2015) exhibit good agreement with JKD except for their most heterogeneous example, which exhibits a resonance behavior (their fig. 7). They consider adding a transient term to the flux equation, which results in a hyperbolic (rather than parabolic) model for mass conservation in porous media (their eq. 21) but fails to explain the entire suite of numerical results. Laboratory experiments by Medina *et al.* (2015) also explore limits to Darcy's law; they show that, for fluids containing suspensions of solids, the linear relationship between fluid flux and pressure gradient that applies for Newtonian fluids breaks down, and strongly heterogeneous velocity fields develop within fractures. Small (3%) variations in solid volume fraction can cause twofold velocity variation.

Selvadurai (2015) explores the influence of stress state (axial normal stress) on the permeability of a single fracture through cylinders of Barre Granite and demonstrates $>10^2$-fold variation in fracture k in response to axial stress ranging from 0–7+ MPa, with k hysteresis ($<10^1$-fold) between loading and unloading cycles. Rutqvist (2015) reviews a variety of field data on stress-induced permeability changes in fractured rock and also discusses the effects of thermally and chemically induced fracture closure; his fig. 14 summarizes fractured rock k to 0.6 km depth at Gidea, Sweden, and his fig. 16 summarizes crystalline bedrock k to 7+ km depth from a variety of sites.

Static permeability

The papers broadly categorized as dealing with static permeability include contributions related to sediments and sedimentary rocks (2 papers) and igneous and metamorphic rocks (4 papers). Volcanic, sedimentary, plutonic, and metamorphic rocks represent about 9%, 73%, 7%, and 11% respectively, of the exposed continental crust (Wilkinson *et al.* 2009). This special issue includes representative publications concerning each of these broad categories. Extensive studies and compilations of permeability in sedimentary rock exist in the petroleum geology literature (e.g. Ehrenberg & Nadeau 2005) and industry archives, but this is not a large emphasis of the special issue. Much of the data in petroleum-industry archives is not publically disclosed, which limits its utility for study, analysis, and modeling. In contrast to the near-surface crust, the bulk of the continental crust is dominated by metamorphic rocks (approximately 90% of crustal volume despite only approximately 10% of surface exposures) rather than sedimentary rock (only a few percent of crustal volume despite approximately 70% of surface exposures) (Wilkinson *et al.* 2009). Much less is known about the permeability of the predominantly metamorphic deeper crust compared with the near-surface crust, as echoed in this special issue by the lack of well-test data from the deeper crust and differing perspectives on the likelihood of Darcian flow below the brittle-ductile transition (BDT) (Yardley 2009; Stober & Bucher, 2015; Connolly & Podladchikov, 2015).

Sediments and sedimentary rocks

Luijendijk & Gleeson (2015) explore porosity–permeability relations for clastic sediments (sand–clay mixtures) to a depth of 2 km, a depth restriction that largely avoids complications such as pressure solution and hydrothermal alteration. They find that the laboratory-scale k of natural sand–clay mixtures is best predicted as the geometric mean of the permeabilities of the sand and clay components and suggest that their algorithm could be applied to well-log data by using neutron and density logs to estimate clay content and porosity (their fig. 9). Daigle & Screaton (2015) explore a large laboratory-scale sediment-permeability data set (530 samples) from ODP and IODP sites worldwide; the emphasis is on the relationship between permeability (10^{-21} to 10^{-14} m^2) and porosity (0.2–0.8) for various subsets of the data. They find that anisotropy is modest (their fig. 8), that field and laboratory k measurements are quite consistent (their fig. 9), and that porosity–permeability trends seem to be maintained through burial and diagenesis to porosity <0.10, suggesting that extrapolation to significant depth is reasonable.

Igneous and metamorphic rocks

Ranjram *et al.* (2015) explore large *in situ* data sets ($n = 977$ from Sweden, Germany, and Switzerland) to assess the depth dependence of the permeability of crystalline rocks in the shallow (≤2.5 km) crust. The complete data set (their fig. 2) does not support a general k-z relation; however, some specific lithologies and tectonic settings display a statistically significant decrease of permeability with depth. Burns *et al.* (2015) demonstrate that regional groundwater flow can explain lower-than-expected heat flow in a thick sequence of highly anisotropic (k_x/k_z ~10^4) continental flood basalts (Columbia River Basalt Group). The limited *in situ* k data are compatible with a steep permeability decrease (approximately 3.5 orders of magnitude) at 0.6–0.9 km depth (their fig. 4) and approximately 40°C (their fig. 5), possibly a result of low-temperature hydrothermal alteration; these authors note that substantial k decreases at similar temperatures have also been observed in the volcanic rocks of the Cascade Range and at Kilauea Volcano, Hawaii. Geochemical analyses and numerical modeling by Pepin *et al.* (2015) suggest that the Truth or Consequences, New Mexico, hot-spring system is supported by deep (2–8 km) circulation in permeable (10^{-12} m^3) crystalline basement rocks. Circulation of meteoric fluids to these depths may occur through ‘hydrologic windows’ in overlying, lower permeability units. Their figure 1 compares basement permeabilities inferred for Rio Grande Rift hydrothermal systems with published k-z curves. Finally, Stober & Bucher (2015) provide a conceptual/qualitative discussion of fluid flow in crystalline rocks above the BDT; their contribution includes observations of decreasing *in situ* k with depth in a single, deep borehole (their fig. 1).

Dynamic permeability

The papers broadly categorized as dealing with the dynamic variability of permeability include contributions related to oceanic crust (1 paper), fault zones (4 papers), crustal-scale phenomena (3 papers), and the effects of fluid injection at the reservoir or ore-deposit scale (3 papers).

Oceanic crust

Cann *et al.* (2015) consider the crystalline crust near the mid-ocean ridge (MOR). They show that alteration of sheeted dikes to episodite ‘stripes’ entails extensive dissolution of primary dike minerals and creates significant transient porosity (≤0.20) and permeability. Each dike was altered before being cut by a later dike, indicating a maximum timescale of 2000 years for hydrothermal alteration. This ‘reaction permeability’ is rarely invoked in models of high-temperature MOR circulation, but may have complemented fracturing to provide the high k required for vigorous circulation. The stripe-like reaction k facilitated and channeled fluid flow, while ongoing hydrothermal alteration conditioned fluid chemistry (metasomatism). The Cann *et al.* contribution is unique (in this collection) in considering the implications of outcrop- to thin section-scale mineralogy and paragenetic sequencing.

Fault zones

Saffer (2015) considers active subduction-zone faults, which are important conduits for dewatering and transport of heat and solutes. He shows that fault-zone permeability values are consistent between margins, with time-averaged values of 10^{-15} to 10^{-14} m^2 and transient values of 10^{-13} to 10^{-11} m^2. Such values are approximately 10^6 times higher than estimated sediment permeabilities at (for instance) 5 km depth (his fig. 6). Permeable zones occupy a small fraction of the fault surface at any one time and migrate over time. Cox *et al.* (2015) show that intermediate- to far-field earthquakes (generating seismic energy densities approximately 0.1 J m^{-3}) cause characteristic 5-day delayed, approximately 1°C cooling of thermal springs in the Southern Alps, New Zealand. They attribute this behavior to permanent strains of 0.1–1 microstrain that open or cause fractures and allow greater mixing between thermal waters and cool groundwater. Micklethwaite *et al.* (2015) focus on underlapping fault stepovers, a type of stepover that is relatively rare but anomalously associated with gold deposits. They model the associated Coulomb failure stress changes and explains the association with gold in terms of localized fault damage. Supergiant gold deposits imply transiently high permeabilities on the order of 10^{-12} m^2, with healing on a timescale of 10^0 to 10^1 years (his fig. 9); a 5 Moz goldfield could perhaps form in 10–1000 years. Howald *et al.* (2015) use the age and isotopic composition of sinter in the (former) Beowawe geyser field to infer two long-lived (5×10^3 year) hydrothermal-discharge events following M < 5 earthquakes on the Malpais fault zone. Simulation of temperature and isotopic composition (their fig. 8) suggest that the earthquakes caused a $>10^3$ increase in k (from $<10^{-14}$ to $>10^{-11}$ m^2).

Crustal-scale behavior

Porosity waves are a mechanism by which fluids can be expelled from ductile rocks below the BDT. Connolly & Podladchikov (2015) present a general, analytical steady-state solution to the hydraulic equation that governs such flow and predicts the dynamic variations in fluid pressure and permeability necessary to accommodate fluid production. Their fig. 8 is a conceptual model of flow regimes from the deep, ductile crust to the surface, and assumes a approximately 10-km-thick transition zone above and below the BDT. Okada *et al.* (2015) show that, following the M_w 9.0 Tohoku earthquake in 2011, earthquake swarms at approximately 4–10 km depth exhibited temporal expansion that can be explained by fluid diffusion (e.g. their fig. 8; note the consistent rates), with inferred $k \sim 5 \times 10^{-16}$ m^2. The M_w 8.0 Wenchuan earthquake in 2008 caused coseismic groundwater-level changes across China. Shi *et al.* (2015) show that the sign and amplitude of water-level response was essentially random; thus, poroelastic response to coseismic static strain was not responsible for most water-level changes, even in the near field. Rather, hydrogeologic and tectonic settings were the dominant controlling factors, and permeability enhancement was the dominant mechanism.

Effects of fluid injection at the scale of a reservoir or ore-deposit

Hydromechanical simulations of fluid injection into the very shallow crystalline crust by Preisig *et al.* (2015) show development of connected permeability to be almost exclusively orthogonal to the minimum principle stress, resulting in strongly anisotropic flow regardless of injection design. This is because tensile opening of a hydraulic fracture generates an increase in stress that limits the response of neighboring fractures in both tensile opening and shear. Whereas most papers in this collection deal with an isotropic permeability (implying $k = k_x = k_y = k_z$) or two primary k orientations (e.g. k_x and k_z), the full permeability tensor is relevant to their analysis (e.g. their eq. 6). Miller (2015) simulates the well-known enhanced geothermal experiment in Basel, Switzerland. He assumes a range of existing fault orientations subject to Mohr–Coulomb failure (his fig. 4) and effective-stress-dependent permeability that increases stepwise (×1000) when a failure criterion is satisfied; assumes a pre-existing permeability distribution; solves a nonlinear form of the diffusion equation (his eq. 5) subject to the observed pressure-time history; catalogs an 'earthquake' when any gridpoint fails; and successfully simulates the time history of permeability evolution (his figs 5 and 6), hypocenter migration (his fig. 9), and earthquake rates (his fig. 10). Finally, Weis (2015) simulates multiphase H_2O–NaCl fluid flow in concert with a dynamic permeability model, isolating (for instance) the influence of NaCl (his figs 7 versus 9) and subaerial topography (figs 10 and 11).

A data structure to integrate and extend existing knowledge

We live in an era of exploding information technology. Thus, the final paper in this collection, by Fan *et al.*, outlines a vision for the 'DigitalCrust': a community-governed, four-dimensional data system of the Earth's crustal structure. The DigitalCrust concept posits a particular emphasis on crustal permeability and porosity, which have not been synthesized elsewhere and play an essential role in crustal dynamics.

TOWARD SYSTEMATIC CHARACTERIZATION

The measured permeability of the shallow continental crust is so highly variable that it is often considered to defy systematic characterization. Nevertheless, some order has been revealed in globally compiled data sets, including postulated relations between permeability and depth on a whole-crust scale (*i.e.* to approximately 30 km depth; e.g. Manning & Ingebritsen 1999; Ingebritsen & Manning 2010) and between permeability and lithology in the uppermost crust (to approximately 100 m depth: Gleeson *et al.* 2011). The recognized limitations of these empirical relations helped to inspire this collection of papers.

In fact, certain papers in this collection highlight the fallacy of extrapolating crustal-scale *k-z* relations to the uppermost crust (e.g. Burns *et al.* 2015; Ranjram *et al.* 2015). The permeability structure of the shallow (approximately <1 km) crust is highly heterogeneous, and dominant controls on local permeability include the primary lithology, porosity, rheology, geochemistry, and tectonic and time-temperature histories of the rocks. The permeability of clastic sediments in the cool, shallow crust is often well predicted as a function of mechanical compaction and consequent porosity–permeability relations (e.g. Daigle & Screaton, 2015; Luijendijk & Gleeson, 2015). However, this predictability diminishes at depths where diagenetic process become important (e.g. Fig. 2a); in the North Sea basin, for instance, pressure solution begins to affect porosity–permeability relations at approximately 2 km depth (Fig. 2b). Similarly, hydrothermal alteration of volcanic rocks tends to cause significant reduction of permeability at temperatures in excess of approximately 40–50°C (e.g. Burns *et al.* 2015). Systematic permeability differences among original lithologies persist to contact-metamorphic depths of 3–10 km, but are not evident at regional metamorphic depths of 10–30+ km (Fig. 3) – presumably because, at greater depths, the metamorphic textures are largely independent of the original lithology.

The temporal evolution of permeability can be gradual or abrupt. Streamflow responses to moderate to large earthquakes demonstrate that dynamic stresses can instantaneously change permeability on a regional scale (e.g. Rojstaczer & Wolf 1992); large (1 mm) fractures can be sealed by silica precipitation within 10 years (Lowell *et al.* 1993); and simulations of calcite dissolution in coastal carbonate aquifers suggest significant changes in porosity and permeability over timescales of 10^4–10^5 years (Sanford & Konikow 1989). At the other end of the spectrum, the reduction of pore volume during sediment burial modifies permeability very slowly. For example, shale permeabilities from the U.S. Gulf Coast vary from about 10^{-18} m^2 near the surface to about 10^{-20} m^2 at 5 km depth (Neglia 1979), and the natural subsidence rate is 0.1–10 mm year^{-1} (Sharp & Domenico 1976), so we can infer that it takes perhaps 10^7 years for the permeability of a subsiding package of shale to decrease by a factor of 10. These various observations are consistent with suggestions that crustal-scale permeability is a dynamically self-adjusting property, reflecting a competition between permeability destruction by processes such as compaction and permeability creation by processes such as fluid sourcing (e.g. Connolly & Podladchikov, 2015) and tectonically driven fracturing and faulting.

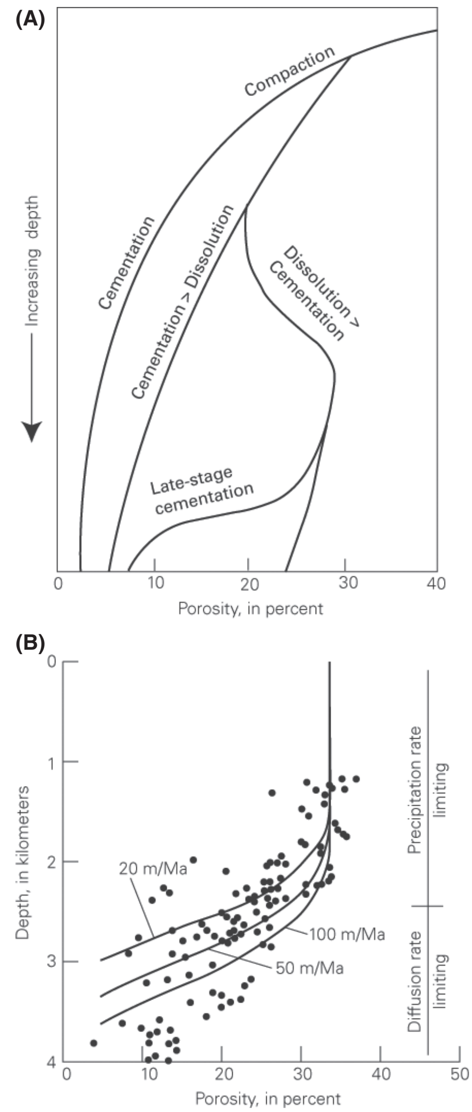

Fig. 2. (a) Hypothetical curves of porosity versus depth in siliciclastic basin sediments, showing the effects of simultaneous compaction, cementation, and dissolution at different rates (after Loucks *et al.* 1984) and (b) porosity-depth variation due to pressure solution in the North Sea. Porosity data are given in Ramm (1992), and the numerical modeling results are given in Renard *et al.* (2000). Calculations are for porosity loss due to pressure solution alone and correspond to three different burial rates.

Nonetheless, given the highly variable rates and scales of permeability creation and decay, considering permeability as static parameter can be a reasonable assumption for a wide range of research problems and applications. For example, for typical low-temperature hydrogeologic investigations with timescales of days to decades, permeability may be considered static in the absence of seismicity. Simi-

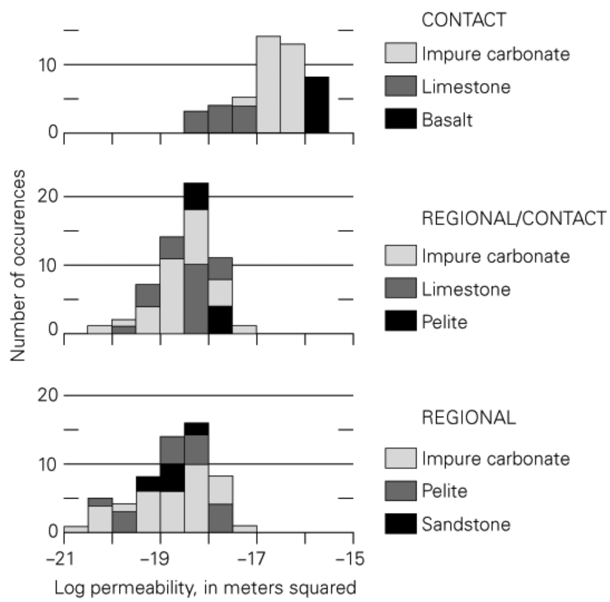

Fig. 3. Histograms of metamorphic permeabilities for contact, regional contact, and regional metamorphic settings, showing differences encountered in different lithologies. 'Regional contact' refers to continental volcanic arcs with elevated geothermal gradients due to heat transported by magma. From Manning & Ingebritsen (1999).

larly, if it takes perhaps 10^7 years for the permeability of a subsiding package of shale to decrease by a factor of 10, permeability in sedimentary basins may be considered static for investigations on much shorter timescales. Whether the dynamic variation of permeability is important to include in analyses and quantitative models depends upon its rapidity and magnitude relative to the requirements of the problem at hand.

Recent research on enhanced geothermal reservoirs, ore-forming systems (Fig. 4), and the hydrologic effects of earthquakes yields broadly consistent results regarding permeability enhancement by dynamic stresses. Shear dislocation caused by tectonic forcing or fluid injection can increase near- to intermediate-field permeability by factors of 100 to 1000. Dynamic stresses (shaking) in the intermediate- to far-field corresponding to seismic energy densities >0.01 J m^{-3} also increase permeability, albeit often by ≪10 and at most by a factor of approximately 20 (e.g. Wang & Manga 2010; Manga *et al.* 2012). These permeability increases are transient, tending to return to preseismic values over timescales on the order of months to decades (e.g. Elkhoury *et al.* 2006; Kitagawa *et al.* 2007; Xue *et al.* 2013). There is reasonable agreement between the magnitude of near- to intermediate-field permeability increases (10^2 to 10^3-fold) directly measured at enhanced geothermal sites (e.g. Evans *et al.* 2005; Häring *et al.* 2008), inferred from field evidence (e.g. Howald *et al.* 2015; Saffer 2015), invoked in simulations of transient hydrothermal circulation (e.g. Weis *et al.* 2012; Taron *et al.* 2014; Howald *et al.* 2015; Weis, 2015), and inferred from seismic and metamorphic data (Ingebritsen & Manning 2010). We note that enhanced geothermal systems, geologic carbon sequestration (Lucier & Zoback

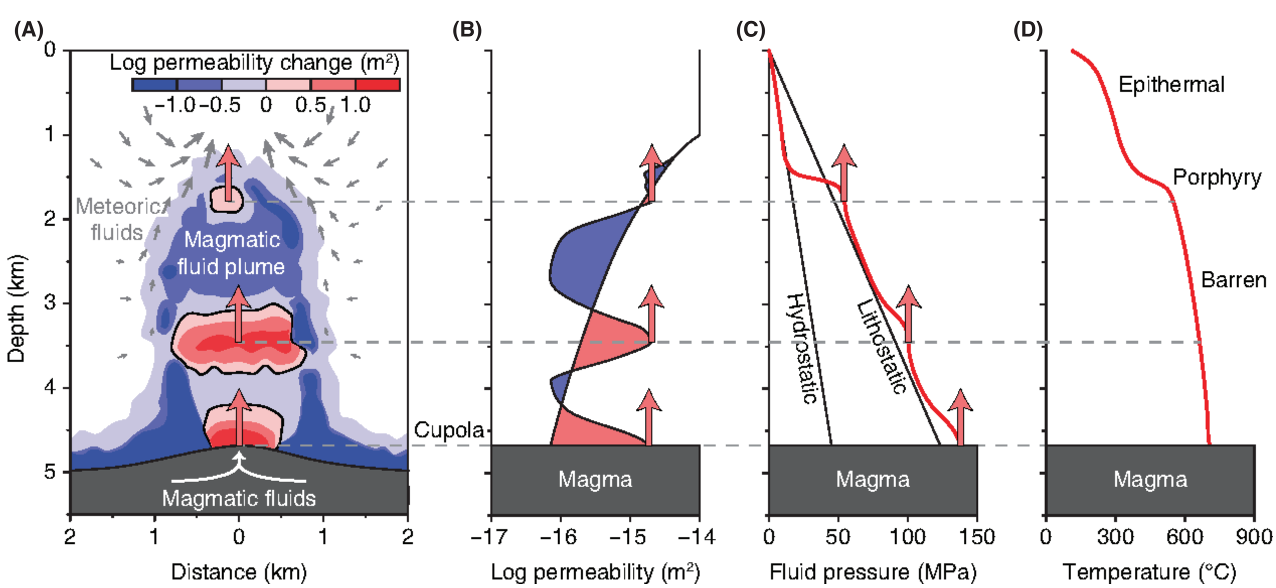

Fig. 4. (a) Simulated porosity/permeability waves driven by injection of magmatic volatiles from a cupola at 5 km depth; wave velocity in this example is approximately 3 km/year. (b) Simulated permeability at any given depth varies by a factor of 10^1 to 10^2 as the waves pass; (c) rock failure is assumed to occur at near-lithostatic fluid pressures below the brittle–ductile transition (BDT) and near-hydrostatic fluid pressures above the BDT. The stable interface between the magmatic fluid plume and meteoric convection seen in (a) acts to localize mineralization (d). After Weis *et al.* (2012; see also Connolly & Podladchikov (2015) and Weis (2015).

2008), and deep injection of waste fluid (Hsieh & Bredehoeft 1981; Frohlich *et al.* 2014) all entail similar stimuli, namely fluid-injection rates on the order of 10 s of kg s^{-1}, as do the simulations of ore-forming systems by Weis (2015). In North America, fluid-injection practices have caused a recent and dramatic increase in $M_w > 3$ seismic events on a nearly continental scale (e.g. Hitzman *et al.* 2012; Ellsworth 2013). This ongoing injection experiment, although poorly constrained, represents an opportunity to explore and assess dynamic crustal permeability to depths of perhaps 10 km.

Even the most intensive campaigns to measure permeability in the very shallow crust cannot yield unambiguous determination of the large-scale trends that govern, for instance, transport behavior (e.g. Eggleston & Rojstaczer 1998). Thus it is likely that models of large-scale fluid transport will continue to depend on inferences based on geophysical imaging and on improved understanding of the thermal, mechanical, and geochemical factors that control the overall permeability structure of the crust. Our hope and expectation is that this collection of papers and the associated data will enhance our ability to quantify or predict permeability and its variability with space, direction, and time.

ACKNOWLEDGEMENTS

We thank the USGS Powell Center for hosting two workshops that led to this collection of papers; the USGS Geothermal and Volcano Hazards programs (SEI) and the National Science and Engineering Research Council (TG); and Erick Burns, Paul Hsieh, Christian Huber, Michael Manga, Craig Manning, Mark Person, and Richard Worden for thoughtful comments that helped to improve this introduction. As Guest Editors, we also thank all authors for their persistence and for their substantial contributions to this special issue of *Geofluids*; the 60 or so referees who helped to evaluate and improve those contributions; and the Editors and staff of *Geofluids* for their advice and support. Articles co-authored by the Guest Editors were handled with editorial independence.

REFERENCES

Baker ET, Massoth GJ, Feely RA (1987) Cataclysmic hydrothermal venting on the Juan de Fuca Ridge. *Nature*, **329**, 149–51.

Bear J (1972) *Dynamics of Fluids in Porous Media*. American Elsevier, New York.

Bear J (1979) *Hydraulics of Groundwater*. McGraw-Hill, New York.

Burns E, Williams CF, Ingebritsen SE, Voss CI, Spane FA, DeAngelo J (2015) Understanding heat and groundwater flow through continental flood basalt provinces: insights gained from alternative models of permeability/depth relationships for the Columbia Plateau, USA. *Geofluids*, **15**, 120–38.

Cann JR, McCaig AM, Yardley BWD (2015) Rapid generation of reaction permeability in the roots of black smoker systems, Troodos ophiolite, Cyprus. *Geofluids*, **15**, 179–92.

Cathles LM, Adams JJ (2005) Fluid flow and petroleum and mineral resources in the upper (<20 km) continental crust. *Economic Geology 100th Anniversary Volume*, 77–110.

Cathles LM, Erendi HJ, Barrie T (1997) How long can a hydrothermal system be sustained by a single intrusive event? *Economic Geology*, **92**, 766–71.

Connolly JAD (1997) Devolatilization-generated fluid pressure and deformation-propagated fluid flow during prograde regional metamorphism. *Journal of Geophysical Research*, **102**, 149–73.

Connolly JAD, Podladchikov VV (2015) An analytical solution for solitary porosity waves: implications for dynamic permeability and fluidization of nonlinear viscous and viscoplastic rock. *Geofluids*, **15**, 269–92.

Cox S, Menzies C, Sutherland R, Denys P, Chamberlain C, Teagle D (2015) Changes in hot spring temperature and hydrogeology of the Alpine Fault hanging wall, New Zealand, induced by South Island earthquakes. *Geofluids*, **15**, 216–39.

Daigle H, Screaton E (2015) Evolution of sediment permeability during burial and subduction. *Geofluids*, **15**, 84–105.

Deming D, Craganu C, Lee Y (2002) Self-sealing in sedimentary basins. *Journal of Geophysical Research*, **107**, ETG 2-1–9.

Eggleston C, Rojstaczer S (1998) Identification of large-scale hydraulic conductivity trends and the influence of trends on contaminant transport. *Water Resources Research*, **34**, 2155–68.

Ehrenberg SN, Nadeau PH (2005) Sandstone vs. carbonate petroleum reservoirs: a global perspective on porosity-depth and porosity-permeability relationships. *AAPG Bulletin*, **89**, 435–45.

Elkhoury JE, Brodsky EE, Agnew DC (2006) Seismic waves increase permeability. *Nature*, **441**, 1135–8.

Ellsworth WL (2013) Injection-induced earthquakes. *Science*, **341**, 142.

Evans KF, Genter A, Sausss J (2005) Permeability creation and damage due to massive fluid injections into granite at 3.5 km at Soultz: 1. Borehole observations. *Journal of Geophysical Research*, **110**, B04203. doi:10.1029/2004JB003168.

Fan Y, Richard S, Bristol RS, Peters SE, Ingebritsen SE, Moosdorf N, Packman A, Gleeson T, Zaslavsky I, Peckham S, Murdoch L, Fienen M, Cardiff M, Tarboton D, Jones N, Hooper R, Arrigo J, Gochis D, Olson J, Wolock D (2015) DigitalCrust – A 4D data system of material properties for transforming research on crustal fluid flow. *Geofluids*, **15**, 372–9.

Fornari DJ, Shank T, Von Damm KL, Gregg TKP, Lilley M, Levai G, Bray A, Haymon RM, Perfit MR, Lutz R (1998) Time-series temperature measurements at high-temperature hydrothermal vents, East Pacific Rise 9°49′-51′N: evidence for monitoring a crustal cracking event. *Earth and Planetary Science Letters*, **160**, 419–31.

Freeze RA, Cherry JA (1979) *Groundwater*. Prentice-Hall, Englewood Cliffs.

Frohlich C, Ellsworth W, Brown WA, Brunt M, Luetgert J, MacDonald T, Walter S (2014) The 17 May 2012 M4.8 earthquake near Timpson, East Texas: an event possibly triggered by fluid injection. *Journal of Geophysical Research Solid Earth*, **119**, 581–93.

Gleeson T, Smith L, Moosdorf N, Hartmann J, Durr HH, Manning AH, van Beek LPH, Jellinek AM (2011) Mapping

permeability over the surface of the Earth. *Geophysical Research Letters*, **38**, L02401.
Hanson RB (1995) The hydrodynamics of contact metamorphism. *Geological Society of America Bulletin*, **107**, 595–611.
Häring MO, Schanz U, Ladner F, Dyer BC (2008) Characterisation of the Basel 1 enhanced geothermal system. *Geothermics*, **37**, 469–95.
Haymon RM (1996) The response of ridge-crest hydrothermal systems to segmented, episodic magma supply. *Geological Society Special Publication*, **118**, 157–68.
Hill DP, Reasenberg PA, Michael A, Arabaz WJ, Beroza G, Brumbaugh D, Brune JN, Castro R, Davis S, dePolo D, Ellsworth WL, Gomberg J, Harmsen S, House L, Jackson SM, Johnston MJS, Jones L, Keller R, Malone S, Mungaia L, Nava S, Pechmann JC, Sanford A, Simpson RW, Smith RB, Stark M, Stickney M, Vidal S, Walter S, Wong V, Zollweg J (1993) Seismicity remotely triggered by the magnitude 7.3 Landers, California, earthquake. *Science*, **260**, 1617–23.
Hitzman MW, many others (Committee on Induced Seismicity Potential in Energy Technologies), (2012) *Induced Seismicity Potential in Energy Technologies.* National Academy Press, Washington, DC.
Howald T, Person M, Campbell A, Lueth V, Hofstra A, Sweetkind D, Gable C, Banerjee A, Luijendijk E, Crossey L, Karlstrom K, Kelley S, Phillips F (2015) Evidence for long-time scale (>10^3 years) changes in hydrothermal activity induced by seismic events. *Geofluids*, **15**, 252–68.
Hsieh PA, Bredehoeft JD (1981) A reservoir analysis of the Denver earthquakes: a case of induced seismicity. *Journal of Geophysical Research*, **86**, 903–20.
Huber C, Su Y (2015) A pore-scale investigation of the dynamic response of saturated porous media to transient stresses. *Geofluids*, **15**, 11–23.
Ingebritsen SE, Manning CE (2002) Diffuse fluid flux through orogenic belts: implications for the world ocean. *Proceedings of the National Academy of Sciences USA*, **99**, 9113–6.
Ingebritsen SE, Manning CE (2010) Permeability of the continental crust: dynamic variations inferred from seismicity and metamorphism. *Geofluids*, **10**, 193–205.
Johnson DL, Koplik J, Dashen R (1987) Theory of dynamic permeability and tortuosity in fluid-saturated porous media. *Journal of Fluid Mechanics*, **176**, 379–402.
Kitagawa Y, Fujimori K, Koizumi N (2007) Temporal change in permeability of the Nojima Fault zone by repeated water injection experiments. *Tectonophysics*, **443**, 183–92.
Loucks RG, Dodge MM, Galloway WE (1984) Regional controls of diagenesis and reservoir quality in Lower Tertiary sandstones along the Texas Gulf Coast. In: *Clastic Diagenesis*, (eds McDonald DA, Surdam RC). *American Association of Petroleum Geologists' Memoir*, **37**, 15–46.
Lowell RP, Van Cappellen P, Germanovich LN (1993) Silica precipitation in fractures and the evolution of permeability in hydrothermal upflow zones. *Science*, **260**, 192–4.
Lucier A, Zoback M (2008) Assessing the economic feasibility of regional deep saline aquifer CO2 injection and storage: a geomechanics-based workflow applied to the Rose Run sandstone in eastern Ohio, USA. *International Journal of Greenhouse Gas Control*, **2**, 230–47.
Luijendijk E, Gleeson T (2015) How well can we predict permeability in sedimentary basins? Deriving porosity-permeability algorithms for non-cemented sand and clay mixtures. *Geofluids*, **15**, B04203, 67–83.
Manga M, Beresnev I, Brodsky EE, Elkhoury JE, Elsworth D, Ingebritsen SE, Mays DC, Wang C-Y (2012) Changes in permeability caused by transient stresses: field observations, experiments, and mechanisms. *Reviews of Geophysics*, **50**, RG2004.
Manning CE, Ingebritsen SE (1999) Permeability of the continental crust: the implications of geothermal data and metamorphic systems. *Reviews of Geophysics*, **37**, 127–50.
Medina R, Elkhoury J, Morris J, Prioul R, Desroches J, Detwiler R (2015) Flow of dense suspensions through fractures: significant in-plane velocity variations caused by small variations in solid concentration. *Geofluids*, **15**, 24–36.
Micklethwaite S, Ford A, Witt W, Sheldon H (2015) The where and how of faults, fluids, and permeability – Insights from fault stepovers, scaling properties, and gold mineralization. *Geofluids*, **15**, 240–51.
Miller S (2015) Modeling enhanced geothermal systems and the essential nature of large-scale changes in permeability at the onset of slip. *Geofluids*, **15**, 338–49.
Moore DE, Lockner DA, Byerlee JD (1994) Reduction of permeability in granite at elevated temperatures. *Science*, **265**, 1558–61.
Morrow C, Lockner D, Moore D, Byerlee J (1981) Permeability of granite in a temperature gradient. *Journal of Geophysical Research*, **86**, 3002–8.
Neglia S (1979) Migration of fluids in sedimentary basins. *American Association of Petroleum Geologists' Bulletin*, **63**, 573–97.
Okada T, 28 others (2015) Hypocenter migration and crustal seismic velocity distribution observed for the inland earthquake swarms induced by the 2011 Tohoku-Oki earthquake in NE Japan: implications for crustal fluid distribution and crustal permeability. *Geofluids*, **15**, 293–309.
Pepin J, Person M, Phillips F, Kelley S, Timmons S, Owens L, Witcher J, Gable C (2015) Deep fluid circulation within crystalline basement rocks and the role of hydrologic windows in the formation of the Truth or Consequences, New Mexico low-temperature geothermal system. *Geofluids*, **15**, 139–60.
Preisig G, Eberhardt E, Gischig V, Roche V, van der Baan M, Valley B, Kaiser P, Duff D, Lowther R (2015) Development of connected rock mass permeability in massive crystalline rocks through hydraulic fracture propagation and shearing accompanying fluid injection. *Geofluids*, **15**, 321–37.
Ramm M (1992) Porosity-depth trends in reservoir sandstones: theoretical models related to Jurassic sandstones, offshore Norway. *Marine and Petroleum Geology*, **9**, 553–67.
Ranjram M, Gleeson T, Luijendijk E (2015) Is the permeability of crystalline rock in the shallow crust related to depth, lithology, or tectonic setting? *Geofluids*, **15**, 106–19.
Renard F, Brosse E, Gratier JP (2000) The different processes involved in the mechanism of pressure-solution in quartz-rich rocks and their interactions. In: *Quartz Cementation of Sandstones*, (eds Worden RH, Morad S). *International Association of Sedimentologists' Special Publication*, **29**, 67–78.
Rojstaczer SA, Wolf S (1992) Permeability changes associated with large earthquakes: an example from Loma Prieta, California. *Geology*, **20**, 211–4.
Rojstaczer SA, Wolf S, Michel R (1995) Permeability enhancement in the shallow crust as a cause of earthquake-induced hydrological changes. *Nature*, **373**, 237–9.
Rojstaczer SA, Ingebritsen SE, Hayba DO (2008) Permeability of continental crust influenced by internal and external forcing. *Geofluids*, **8**, 128–39.
Rutqvist J (2015) Fractured rock stress-permeability relationships from *in situ* data and the effects of temperature and chemical-mechanical couplings. *Geofluids*, **15**, 48–66.

Saffer D (2015) The permeability of active subduction plate boundary faults. *Geofluids*, **15**, 193–215.

Sanford WE, Konikow LF (1989) Simulation of calcite dissolution and porosity changes in salt water mixing zones in coastal aquifers. *Water Resources Research*, **25**, 655–67.

Selvadurai P (2015) Normal stress-induced permeability hysteresis of a fracture in a granite cylinder. *Geofluids*, **15**, 37–47.

Sharp JM Jr, Domenico PA (1976) Energy transport in thick sequences of compacting sediment. *Geological Society of America Bulletin*, **87**, 390–400.

Shi Z, Wang G, Manga M, Wang C-Y (2015) Continental-scale water-level response to a large earthquake. *Geofluids*, **15**, 310–20.

Sibson RH, Moore JMM, Rankin AH (1975) Seismic pumping – A hydrothermal fluid transport mechanism. *Journal of the Geological Society of London*, **131**, 653–9.

Sohn RA (2007) Stochastic analysis of exit fluid temperature records from the active TAG hydrothermal mound (Mid-Atlantic Ridge, 26°N): 1. Modes of variability and implications for subsurface flow. *Journal of Geophysical Research*, **112**, B07101, doi:10.1029/2006JB004435.

Stober I, Bucher K (2015) Hydraulic conductivity of fractured upper crust: insights from hydraulic tests in boreholes and fluid-rock interaction in crystalline basement rocks. *Geofluids*, **15**, 161–78.

Taron J, Hickman S, Ingebritsen SE, Williams C (2014) Using a fully coupled, open-source THM simulator to examine the role of thermal stresses in shear stimulation of enhanced geothermal systems. 48th US Rock Mechanics/Geomechanics Symposium, Minneapolis, Minnesota, 1–4 June 2014, ARMA 14-7525, 10 p.

Townend J, Zoback MD (2000) How faulting keeps the crust strong. *Geology*, **28**, 399–402.

Walder J, Nur A (1984) Porosity reduction and crustal pore pressure development. *Journal of Geophysical Research*, **89**, 11539–48.

Wang CY, Manga M (2010) *Earthquakes and Water*. Springer-Verlag, Berlin, Heidelberg, pp. 225. (Lecture Notes in Earth Sciences 114)

Weis P (2015) The dynamic interplay between saline fluid flow and rock permeability in magmatic-hydrothermal systems. *Geofluids*, **15**, 350–71.

Weis P, Driesner T, Heinrich CA (2012) Porphyry-copper ore shells form at stable pressure-temperature fronts within dynamic fluid plumes. *Science*, **338**, 1613–6.

Wilkinson BH, McElroy BJ, Kesler SE, Peters SE, Rothman ED (2009) Global geologic maps are tectonic speedometers – rates of rock cycling from area-age frequencies. *Geological Society of America Bulletin*, **121**, 760–79.

Winograd IJ (1971) Hydrogeology of ash-flow tuff: a preliminary statement. *Water Resources Research*, **7**, 994–1006.

Xue L, Li H-B, Brodsky EE, Xu Z-Q, Kano Y, Wang H, Mori JJ, Si J-L, Pei J-L, Zhang W, Yang G, Sun Z-M, Huang Y (2013) Continuous permeability measurements record healing inside the Wenchuan earthquake fault zone. *Science*, **340**, 1555–9.

Yardley BWD (1986) Fluid migration and veining in the Connemara Schists. In: *Fluid-Rock Reactions During Metamorphism, Advances in Physical Geochemistry, 5*, (eds Walther JV, Wood BJ), pp. 109–31. Springer-Verlag, New York.

Yardley BWD (2009) The role of water in the evolution of the continental crust. *Journal of the Geological Society*, **166**, 585–600.

Yasuhara H, Polak A, Mitani Y, Grader AS, Halleck PM, Elsworth D (2006) Evolution of fracture permeability through fluid-rock reaction under hydrothermal conditions. *Earth and Planetary Science Letters*, **244**, 186–200.

GEOFLUIDS

Volume 15, Number 1 and 2, February 2015

ISSN 1468-8115

CONTENTS

INTRODUCTION TO THE SPECIAL ISSUE ON CRUSTAL PERMEABILITY

1 **Crustal permeability: Introduction to the special issue**
S.E. Ingebritsen and T. Gleeson

THE PHYSICS OF PERMEABILITY

11 **A pore-scale investigation of the dynamic response of saturated porous media to transient stresses**
C. Huber and Y. Su

24 **Flow of concentrated suspensions through fractures: small variations in solid concentration cause significant in-plane velocity variations**
R. Medina, J.E. Elkhoury, J.P. Morris, R. Prioul, J. Desroches and R.L. Detwiler

37 **Normal stress-induced permeability hysteresis of a fracture in a granite cylinder**
A.P.S. Selvadurai

48 **Fractured rock stress-permeability relationships from in situ data and effects of temperature and chemical-mechanical couplings**
J. Rutqvist

STATIC PERMEABILITY

Sediments and sedimentary rocks

67 **How well can we predict permeability in sedimentary basins? Deriving and evaluating porosity–permeability equations for noncemented sand and clay mixtures**
E. Luijendijk and T. Gleeson

84 **Evolution of sediment permeability during burial and subduction**
H. Daigle and E.J. Screaton

Igneous and metamorphic rocks

106 **Is the permeability of crystalline rock in the shallow crust related to depth, lithology or tectonic setting?**
M. Ranjram, T. Gleeson and E. Luijendijk

120 **Understanding heat and groundwater flow through continental flood basalt provinces: insights gained from alternative models of permeability/depth relationships for the Columbia Plateau, USA**
E.R. Burns, C.F. Williams, S.E. Ingebritsen, C.I. Voss, F.A. Spane and J. Deangelo

139 **Deep fluid circulation within crystalline basement rocks and the role of hydrologic windows in the formation of the Truth or Consequences, New Mexico low-temperature geothermal system**
J. Pepin, M. Person, F. Phillips, S. Kelley, S. Timmons, L. Owens, J. Witcher and C. Gable

161 **Hydraulic conductivity of fractured upper crust: insights from hydraulic tests in boreholes and fluid-rock interaction in crystalline basement rocks**
I. Stober and K. Bucher

DYNAMIC PERMEABILITY

Oceanic crust

179 **Rapid generation of reaction permeability in the roots of black smoker systems, Troodos ophiolite, Cyprus**
J.R. Cann, A.M. McCaig and B.W.D. Yardley

Fault zones

193 **The permeability of active subduction plate boundary faults**
D.M. Saffer

216 **Changes in hot spring temperature and hydrogeology of the Alpine Fault hanging wall, New Zealand, induced by distal South Island earthquakes**
S.C. Cox, C.D. Menzies, R. Sutherland, P.H. Denys, C. Chamberlain and D.A.H. Teagle

240 **The where and how of faults, fluids and permeability – insights from fault stepovers, scaling properties and gold mineralisation**
S. Micklethwaite, A. Ford, W. Witt and H.A. Sheldon

252 **Evidence for long timescale (>10^3 years) changes in hydrothermal activity induced by seismic events**
T. Howald, M. Person, A. Campbell, V. Lueth, A. Hofstra, D. Sweetkind, C.W. Gable, A. Banerjee, E. Luijendijk, L. Crossey, K. Karlstrom, S. Kelley and F.M. Phillips

Crustal-scale-behaviour

269 **An analytical solution for solitary porosity waves: dynamic permeability and fluidization of nonlinear viscous and viscoplastic rock**
J.A.D. Connolly and Y.Y. Podladchikov

293 **Hypocenter migration and crustal seismic velocity distribution observed for the inland earthquake swarms induced by the 2011 Tohoku-Oki earthquake in NE Japan: implications for crustal fluid distribution and crustal permeability**
T. Okada, T. Matsuzawa, N. Umino, K. Yoshida, A. Hasegawa, H. Takahashi, T. Yamada, M. Kosuga, T. Takeda, A. Kato, T. Igarashi, K. Obara, S. Sakai, A. Saiga, T. Iidaka, T. Iwasaki, N. Hirata, N. Tsumura, Y. Yamanaka, T. Terakawa, H. Nakamichi, T. Okuda, S. Horikawa, H. Katao, T. Miura, A. Kubo, T. Matsushima, K. Goto and H. Miyamachi

310 **Continental-scale water-level response to a large earthquake**
Z. Shi, G. Wang, M. Manga and C.-Y. Wang

Effects of fluid injection at the scale of a reservoir or ore deposit

321 **Development of connected permeability in massive crystalline rocks through hydraulic fracture propagation and shearing accompanying fluid injection**
G. Preisig, E. Eberhardt, V. Gischig, V. Roche, M. Van Der Baan, B. Valley, P.K. Kaiser, D. Duff and R. Lowther

338 **Modeling enhanced geothermal systems and the essential nature of large-scale changes in permeability at the onset of slip**
S.A. Miller

350 **The dynamic interplay between saline fluid flow and rock permeability in magmatic-hydrothermal systems**
P. Weis

A DATA STRUCTURE TO INTEGRATE AND EXTEND EXISTING KNOWLEDGE

372 **DigitalCrust – a 4D data system of material properties for transforming research on crustal fluid flow**
Y. Fan, S. Richard, R.S. Bristol, S.E. Peters, S.E. Ingebritsen, N. Moosdorf, A. Packman, T. Gleeson, I. Zaslavsky, S. Peckham, L. Murdoch, M. Fienen, M. Cardiff, D. Tarboton, N. Jones, R. Hooper, J. Arrigo, D. Gochis, J. Olson and D. Wolock